

## Article

# Cyanide Anion Determination Based on Nucleophilic Addition to 6-[(E)-(4-Nitrophenyl)diazenyl]-1',3,3',4-tetrahydrospiro[chromene-2,2'-indole] Derivatives

Miglė Dagilienė<sup>1</sup>, Giedrė Markuckaitė<sup>2</sup> , Sonata Krikštolaitytė<sup>2</sup>, Algirdas Šačkus<sup>1</sup> and Vytas Martynaitis<sup>2,\*</sup> 

<sup>1</sup> Institute of Synthetic Chemistry, Kaunas University of Technology, K. Baršausko g. 59, LT-51423 Kaunas, Lithuania; migle.burinskaite@ktu.lt (M.D.); algirdas.sackus@ktu.lt (A.Š.)

<sup>2</sup> Department of Organic Chemistry, Kaunas University of Technology, Radvilėnų pl. 19, LT-50254 Kaunas, Lithuania; markuckaite.giedre@gmail.com (G.M.); sonata.krikstolaityte@ktu.lt (S.K.)

\* Correspondence: vyttas.martynaitis@ktu.lt; Tel.: +370-616-33645

**Abstract:** This work provides a novel approach for the instant detection of CN<sup>−</sup> anions based on chromogenic 6-[(E)-(4-nitrophenyl)diazenyl]-1',3,3',4-tetrahydrospiro[chromene-2,2'-indole] derivatives. New colorimetric detectors were synthesized and characterized. These compounds exhibited a substantial color change from orange to magenta and blue when treated with cyanide ions in a CH<sub>3</sub>CN solution buffered with sodium phosphate and demonstrated high selectivity to CN<sup>−</sup> anions. Common anions were tested, and they did not interfere with cyanide detection, except for carbonates and hydrosulfites. The simple preparation of a molecular sensor and the easily noticeable color change makes this a practical system for the monitoring of CN<sup>−</sup> ions. This color change is explained by nucleophilic substitution of the pyrane ring oxygen atom at the indoline C-2 atom by the cyanide anion. This generates the appearance of intensively colored 4-(4-nitrophenylazo)phenolate chromophore and allows for determining very low levels of CN<sup>−</sup> anion.

**Keywords:** spiro[chroman-2,2'-indole]; cyanide determination; colorimetry



**Citation:** Dagilienė, M.; Markuckaitė, G.; Krikštolaitytė, S.; Šačkus, A.; Martynaitis, V. Cyanide Anion Determination Based on Nucleophilic Addition to 6-[(E)-(4-Nitrophenyl)diazenyl]-1',3,3',4-tetrahydrospiro[chromene-2,2'-indole] Derivatives. *Chemosensors* **2022**, *10*, 185. <https://doi.org/10.3390/chemosensors10050185>

Academic Editor: Jun Wang

Received: 9 April 2022

Accepted: 12 May 2022

Published: 14 May 2022

**Publisher's Note:** MDPI stays neutral with regard to jurisdictional claims in published maps and institutional affiliations.



**Copyright:** © 2022 by the authors. Licensee MDPI, Basel, Switzerland. This article is an open access article distributed under the terms and conditions of the Creative Commons Attribution (CC BY) license (<https://creativecommons.org/licenses/by/4.0/>).

## 1. Introduction

Cyanides (as hydrogen cyanide gas or cyanide salts) are very toxic in any form to all aerobic organisms. Cyanide anion has a similar electronic structure to carbon monoxide, and they easily penetrate through biological barriers into the blood system. Cyanides are non-competitive inhibitors of cytochrome c oxidase and bind to heme iron atoms to make a not dissociable complex, leading to the chemical asphyxiation of cells [1]. Cyanides occur not only from cyanide containing industrial waste, air pollution, chimneys of power plants, or vehicle exhaust, but they are also formed during metabolic processes of bacteria, fungi, and algae. Cyanides can release during the ingestion of some food containing glycosides (such as cassava root, apricot seeds, and bitter almonds) [2,3]. Cyanide exposure also occurs relatively frequently in patients who inhale the smoke from industrial or residential fires [4]. Therefore, the development of a detection method that can trace cyanide ions in food analysis and during environmental monitoring has attracted much attention. A few detection strategies have been applied in cyanide ion recognition. Most of these methods not only require expensive equipment, complex preprocessing, and specialists, but they are also time-consuming. Furthermore, they cannot achieve real-time detection, which creates an important disadvantage for cyanide ion detection. Optical sensors for cyanide, in which a change in color and/or fluorescence intensity (or emission wavelength) is monitored, appear to be one of the most convenient methods and have been actively studied over the past twenty years [5–8]. Nevertheless, these sensors often suffer from several drawbacks, such as their complex structure, difficult synthesis, poor selectivity (especially in the presence of fluoride [9] or acetate ions), and their loss of efficacy in protic solvents [10,11]. For this reason,

the development of a reliable, efficient, and selective method for the real-time determination of  $\text{CN}^-$  still retains its relevance. Colorimetric-based sensing has been shown to be unique, as it provides naked-eye detection of the analyte and does not require expensive equipment. Since cyanide ions have strong nucleophilic properties, most reactions that are based on optical detection rely on a nucleophilic addition. Ren et al. [12] discovered that the indolo [2,1-*b*][1,3] benzoxazine derivative undergoes C-O bond cleavage in the oxazine ring upon treatment with cyanide, which is accompanied by the formation of 4-nitrophenolate chromophore and the appearance of a yellowish color, suggesting a potential application for cyanide detection. It was also found that the spiropyran derivative 6-nitro BIPS, which is well known for its photochromic properties, also behaves as a selective and sensitive cyanide anion receptor in aqueous media under UV irradiation [13]. This sensor is converted to its colored merocyanine form upon UV irradiation and when the cyanide anion is the merocyanine- $\text{CN}^-$  adduct that is formed, causing the creation of a new absorption band in the absorption spectrum. Generally, the design of colorimetric receptors is based on the receptor–chromophore conjugate, which involves the binding of a specific analyte with a receptor site and a chromophore that is responsible for translating the receptor–analyte binding into an optical signal. Azo dyes are known for their chromophoric strength, ease of preparation, good price, and coverage of the full color and shade spectrum, thus serving as common chromophores for the target chemosensors, which have been reviewed comprehensively [14–17]. Wang and Kim reported a colorimetric chemodosimeter based on a spiropyran–azosalicylal conjugated structure that requires more than 10 min for the cyanide ion nucleophilic addition reaction to take place at room temperature and less time when it is under high-temperature conditions [18]. Raymo et al. [19,20] showed that indolo[2,1-*b*][1,3][1,3]benzoxazines that possess 4-nitrophenylazo moiety and that form 4-(4-nitrophenyldiazenyl)phenolate chromophore when treated with cyanide ions create absorption bands at 575 nm and also is a potential chemosensor for cyanide detection. However, in this case, if no phase transfer catalysis is used, then the acetonitrile solution of the compound responds to aqueous cyanide solutions with detectable absorbance changes only if the cyanide concentration is greater than 0.1 mM.

In this work, we present a new potential chemosensor that is based on spiro[chroman-2,2'-indole] derivatives for spectrophotometric or naked-eye visual cyanide detection, which is easily synthesized, very fast, sensitive, and selective and that requires no special equipment.

## 2. Materials and Methods

Reagents and solvents were purchased from Sigma-Aldrich and used without purification. Indolium salts **5a** [21], **5b** [22] and **5c** [23] were prepared according to the literature, respectively. Compound **3a** was prepared as described [20]. Water was doubly distilled. Anionic solutions for selectivity testing were prepared from various sodium salts.

TLC analysis was performed using precoated silica gel plates (Kieselgel 87 60F254, Merck, Darmstadt, Germany). For the visualization of compounds on the plates, UV light and spraying with a 1%  $\text{KMnO}_4$  solution were used. Silica gel SI 60 (43–60  $\mu\text{m}$ , E. Merck, Darmstadt, Germany) was used for column chromatography.

Semi-preparative HPLC purification was performed on Shimadzu HPLC system using YMC–Actus Triart C18 column (150  $\times$  20.0 mm I.D., 5  $\mu\text{m}$ ) and gradient conditions from 70/30% water/acetonitrile to 0/100% in 13 min and 100% acetonitrile from 13 to 23 min, 8 mL/min flow-rate, 36  $^\circ\text{C}$ . Büchi B-540 melting point apparatus was used for determination of melting points, and they were uncorrected. Perkin Elmer Spectrum One spectrometer was used to record IR spectra from potassium bromide pellets.  $^1\text{H}$  NMR spectra were recorded at 400 MHz and  $^{13}\text{C}$  NMR spectra—at 100 MHz on a Bruker Avance III spectrometer. Chemical shifts are presented in ppm downfield relative to TMS and coupling constants (J), are expressed in Hz. PerkinElmer spectrometer Lambda 35 was used for recording UV–Vis spectra using quartz cells with a light path length of 0.5 cm. Shimadzu LCMS-2020 system was used for recording mass spectra. Bruker maXis spectrometer

(Bruker, Bremen, Germany) was used for recording high-resolution ESI-TOF mass spectra. Elemental Analyzer CE-440 (Exeter Analytical, Inc, North Chelmsford, MA, USA) was used for determination of elemental compositions by Microanalytical Laboratory, Department of Organic Chemistry, Kaunas University of Technology.

### 2.1. Synthetic Procedures

#### 2.1.1. 4-[(E)-2-Chloro-4'-nitrophenyl]diazenyl-2-hydroxymethylphenol (**3b**)

To a stirred solution of 2-chloro-4-nitroaniline (8.629 g, 50 mmol) in HCl (13%, 50 mL) approx. 50 g of ice was added. Mixture was cooled in an ice bath to 0 °C and maintained at this temperature while a solution of NaNO<sub>2</sub> (3.5 g, 50 mmol) in H<sub>2</sub>O (20 mL) was added by drops for 30 min. The mixture was stirred for a further 30 min and during this time, the temperature was allowed to rise to ambient. The obtained solution of diazonium salt was then added dropwise to a solution of 2-hydroxybenzyl alcohol (6.2 g, 50 mmol) in aqueous NaOH (4%, 75 mL) maintained at 0 °C. The mixture was stirred for a further 1 h, allowing the temperature to rise to ambient. The resultant crystalline material was filtered, washed with cold H<sub>2</sub>O (30 mL), and dried in vacuo to afford the title compound **3b** as orange crystals, yield 12.4 g (80%), which was used for further reaction without purification. A total of 25 mg of the obtained material was purified by semi-preparative HPLC for NMR, HRMS, and IR analysis. mp 169–170 °C. Rt = 12 min. <sup>1</sup>H NMR (400 MHz, CDCl<sub>3</sub>): δ 3.35 (br.s, 1H, OH), 4.55 (s, 2H, CH<sub>2</sub>), 7.01 (d, J = 8.5 Hz, 1H, 6'-H), 7.78 (d, J = 8.9 Hz, 1H, 6-H), 7.82 (dd, J = 8.5, 2.6 Hz, 1H, 5'-H), 8.03 (d, J = 2.6 Hz, 1H, 3'-H), 8.28 (dd, J = 8.9, 2.5 Hz, 1H, 5-H), 8.48 (d, J = 2.5 Hz, 1H, 3-H), 10.26 (br.s, 1H, OH<sub>Ph</sub>). <sup>13</sup>C NMR (100 MHz, CDCl<sub>3</sub>): δ 57.7, 115.3, 118.6, 121.7, 123.5, 125.8, 126.2, 130.6, 132.9, 145.8, 147.8, 152.0, 159.8 (see Figures S1 and S2 in supplementary file). IR (cm<sup>-1</sup>): 3097, 2957, 1517 (NO<sub>2</sub>-asymm.), 1338 (NO<sub>2</sub>-symm.) HRMS (ESI TOF): [M+Na]<sup>+</sup> found 330.0250. [C<sub>13</sub>H<sub>10</sub>ClN<sub>3</sub>NaO<sub>4</sub>]<sup>+</sup> requires 330.0252.

#### 2.1.2. General Procedure for Preparation of **4**

To a stirred solution of the corresponding alcohol (**3a**, **3b**) (2 mmol) in ethyl acetate (10 mL), concentrated hydrochloric acid (2 mL) was added. The mixture was stirred at 70 °C for 4 h. After cooling to room temperature, the solvent was removed under reduced pressure, the residue was dissolved in ethanol (15 mL), poured into water (60 mL), and extracted with diethyl ether (3 × 20 mL). The combined organic phase was washed with water (2 × 30 mL), dried over anhydrous sodium sulfate and the solvent was evaporated under reduced pressure to afford the corresponding alkylating agent (**4a** and **4b**, respectively), as dark red resinous material, which was used for further reaction without purification.

#### 2.1.3. General Procedure for Synthesis of **7**

Corresponding iodide (**5a–c**) (5 mmol) was dissolved in distilled water (15 mL), sodium carbonate (1.06 g, 10 mmol) was added, and the mixture was stirred until it became turbid. The separated substance was extracted with diethyl ether (3 × 20 mL) and combined organic phase was dried over anhydrous sodium sulfate. The ether was removed under reduced pressure yielding corresponding 2-methylene-2,3-dihydro-1H-indole (**6a–c**), respectively, as a brownish oil in case of **6a,b** and bright green solid in case of **6c**. The obtained by such way crude intermediate enamine (**6a–c**) was dissolved in acetonitrile (3 mL) and solution of alkylating agent **4a** or **4b** (5 mmol) in acetonitrile (15 mL) was added to the solution. The mixture was stirred at rt for 4 h. The resultant crystal-like material was filtered, washed with cold acetonitrile (1 mL) and dried in vacuo. Solvent of the filtrate was evaporated under reduced pressure. The residue was subjected to flash chromatography on silica gel (hexane/acetone 10:1, v/v), combined with crystalline material, which first crystallized from the reaction mixture and recrystallized from acetonitrile to afford the title compound (**7a–f**).

1',3',3'-Trimethyl-6-[(E)-(4-nitrophenyl)diazenyl]-1',3,3',4-tetrahydrospiro[chromene-2,2'-indole] (**7a**): Rf = 0.15 (hexane/acetone 10:1, v/v), orange crystals, yield 1.005 g (47%).

mp 219–220 °C.  $^1\text{H}$  NMR (400 MHz,  $\text{CDCl}_3$ ):  $\delta$  1.28 (s, 6H,  $2 \times 3'$ - $\text{CH}_3$ ), 2.33–2.43 (m, 2H, 3- $\text{CH}_2$ ), 2.88 (s, 3H, N- $\text{CH}_3$ ), 3.01–3.24 (m, 2H, 4- $\text{CH}_2$ ), 6.60 (d,  $J = 7.6$  Hz, 1H,  $7'$ -H), 6.85 (d,  $J = 7.8$  Hz, 1H, 8-H), 6.86 (t,  $J = 7.6$  Hz, 1H  $6'$ -H), 7.06 (d,  $J = 7.6$  Hz, 1H,  $4'$ -H), 7.20 (t,  $J = 7.6$  Hz, 1H,  $5'$ -H), 7.77 (d,  $J = 7.8$  Hz, 1H, 7-H), 7.78 (s, 1H, 5H), 7.96 (d,  $J = 8.8$  Hz, 2H,  $2''$ -H,  $6''$ -H), 8.35 (d,  $J = 8.8$  Hz, 2H,  $3''$ -H,  $5''$ -H).  $^{13}\text{C}$  NMR (100 MHz,  $\text{CDCl}_3$ ):  $\delta$  22.0, 23.6, 24.5, 25.7, 28.6, 49.6, 103.7, 107.2, 117.4, 119.2, 121.4, 121.8, 123.1 ( $2 \times \text{C}$ ), 124.2, 124.87 ( $2 \times \text{C}$ ), 124.90, 128.0, 137.3, 146.3, 148.2, 148.8, 156.3, 160.7 (Figures S3 and S4 in Supplementary file). IR ( $\text{cm}^{-1}$ ): 3048, 2967, 1520 ( $\text{NO}_2$ -asymm.), 1341 ( $\text{NO}_2$ -symm.). Anal. Calcd for  $\text{C}_{25}\text{H}_{24}\text{N}_4\text{O}_3$  (428.48): C 70.08; H 5.65; N 13.08. Found: C 69.65; H 5.24; N 13.64. HRMS (ESI TOF):  $[\text{M} + \text{H}]^+$  found 429.1925.  $[\text{C}_{25}\text{H}_{25}\text{N}_4\text{O}_3]^+$  requires 429.1921.

6-[(E)-(2-Chloro-4-nitrophenyl)diazenyl]-1',3',3'-trimethyl-1',3,3',4-tetrahydrospiro[chromene-2,2'-indole] (7b): Rf = 0.15 (hexane/acetone 10:1,  $v/v$ ), dark brown crystals, yield 1.412 g (61%). mp 190–191 °C.  $^1\text{H}$  NMR (400 MHz,  $\text{CDCl}_3$ ):  $\delta$  1.28 (s, 6H,  $2 \times 3'$ - $\text{CH}_3$ ), 2.34–2.44 (m, 2H, 3- $\text{CH}_2$ ), 2.88 (s, 3H, N- $\text{CH}_3$ ), 2.99–3.24 (m, 2H, 4- $\text{CH}_2$ ), 6.60 (d,  $J = 7.6$  Hz, 1H,  $7'$ -H), 6.84 (d,  $J = 7.6$  Hz, 1H,  $6'$ -H), 6.87 (d,  $J = 9.2$  Hz, 1H, 8-H), 7.06 (d,  $J = 7.6$  Hz, 1H,  $4'$ -H), 7.20 (t,  $J = 7.6$  Hz, 1H,  $5'$ -H), 7.75 (d,  $J = 8.9$  Hz, 1H,  $6''$ -H), 7.81 (s, 1H, 5-H), 7.82 (d,  $J = 9.2$  Hz, 1H, 7-H), 8.18 (dd,  $J = 8.9$ , 2.2 Hz, 1H,  $5''$ -H), 8.42 (d,  $J = 2.2$  Hz, 1H,  $3''$ -H).  $^{13}\text{C}$  NMR (100 MHz,  $\text{CDCl}_3$ ):  $\delta$  22.1, 23.6, 24.5, 25.8, 28.6, 49.6, 104.0, 107.3, 117.5, 118.4, 119.3, 121.4, 122.0, 122.8, 125.0, 125.3, 126.2, 128.0, 134.8, 137.2, 146.8, 148.1, 148.8, 152.8, 161.2 (Figures S5 and S6 in Supplementary file). IR ( $\text{cm}^{-1}$ ): 3095, 2961, 1520 ( $\text{NO}_2$ -asymm.), 1344 ( $\text{NO}_2$ -symm.). Anal. Calcd for  $\text{C}_{25}\text{H}_{23}\text{ClN}_4\text{O}_3$  (462.93): C 64.86; H 5.01; N 12.10. Found: C 64.19; H 10.10; N 12.44. HRMS (ESI TOF):  $[\text{M} + \text{H}]^+$  found 463.1536.  $[\text{C}_{25}\text{H}_{24}\text{ClN}_4\text{O}_3]^+$  requires 463.1532.

5'-Methoxy-1',3',3'-trimethyl-6-[(E)-(4-nitrophenyl)diazenyl]-1',3,3',4-tetrahydrospiro[chromene-2,2'-indole] (7c): Rf = 0.31 (hexane/acetone 10:1,  $v/v$ ), dark brown crystals, yield 0.183 g (19%), mp 195–196 °C.  $^1\text{H}$  NMR (400 MHz,  $\text{CDCl}_3$ ):  $\delta$  1.27 (s, 6H,  $2 \times 3'$ - $\text{CH}_3$ ), 2.30–2.43 (m, 2H, 3- $\text{CH}_2$ ), 2.83 (s, 3H, N- $\text{CH}_3$ ), 2.99–3.20 (m, 2H, 4- $\text{CH}_2$ ), 3.79 (s, 3H, O- $\text{CH}_3$ ), 6.50 (d,  $J = 8$  Hz, 1H,  $7'$ -H), 6.66–6.78 (m, 2H,  $4'$ -H,  $6'$ -H), 6.87 (d,  $J = 9.2$  Hz, 1H, 8-H), 7.72–7.81 (m, 2H, 5-H, 7-H), 7.96 (d,  $J = 9.2$  Hz, 2H,  $2''$ -H,  $6''$ -H), 8.35 (d,  $J = 8.8$  Hz, 2H,  $3''$ -H,  $5''$ -H).  $^{13}\text{C}$  NMR (100 MHz,  $\text{CDCl}_3$ ):  $\delta$  22.0, 23.6, 24.6, 25.7, 29.0, 49.8, 56.1, 104.3, 107.4, 109.5, 111.7, 117.4, 121.9, 123.1 ( $2 \times \text{C}$ ), 124.2, 124.86 ( $2 \times \text{C}$ ), 124.91, 138.8, 143.1, 146.3, 148.2, 153.9, 156.3, 160.7 (Figures S7 and S8 in Supplementary file). IR ( $\text{cm}^{-1}$ ): 3076, 2965, 1518 ( $\text{NO}_2$ -asymm.), 1345 ( $\text{NO}_2$ -symm.). MS  $m/z$  (%): 459 ( $\text{M} + \text{H}^+$ , 100). Anal. Calcd for  $\text{C}_{26}\text{H}_{26}\text{N}_4\text{O}_4$  (458.51): C 68.11, H 5.72, N 12.22. Found: C 68.37, H 6.04, N 12.39. HRMS (ESI TOF):  $[\text{M} + \text{H}]^+$  found 459.2024.  $[\text{C}_{26}\text{H}_{27}\text{N}_4\text{O}_4]^+$  requires 459.2027.

6-[(E)-(2-Chloro-4-nitrophenyl)diazenyl]-5'-methoxy-1',3',3'-trimethyl-1',3,3',4-tetrahydrospiro[chromene-2,2'-indole] (7d): Rf = 0.31 (hexane/acetone 10:1,  $v/v$ ), dark brown crystals, yield 0.444 g (18%), mp. 175–176 °C.  $^1\text{H}$  NMR (400 MHz,  $\text{CDCl}_3$ ):  $\delta$  1.27 (s, 6H,  $2 \times 3'$ - $\text{CH}_3$ ), 2.29–2.44 (m, 2H, 3- $\text{CH}_2$ ), 2.83 (s, 3H, N- $\text{CH}_3$ ), 2.99–3.22 (m, 2H, 4- $\text{CH}_2$ ), 3.79 (s, 3H, O- $\text{CH}_3$ ), 6.50 (d,  $J = 8.4$  Hz, 1H,  $7'$ -H), 6.71 (d,  $J = 2.6$  Hz, 1H,  $4'$ -H), 6.74 (dd,  $J = 8.4$  Hz,  $J = 2.6$  Hz, 1H,  $6'$ -H), 6.87 (d,  $J = 9.2$  Hz, 1H, 8-H), 7.75 (d,  $J = 8.8$  Hz, 1H,  $6''$ -H), 7.80 (s, 1H, 5-H), 7.81 (d,  $J = 9.2$  Hz, 1H, 7-H), 8.18 (dd,  $J = 8.8$  Hz,  $J = 2.4$  Hz, 1H,  $5''$ -H), 8.42 (d,  $J = 2.4$  Hz, 1H,  $3''$ -H).  $^{13}\text{C}$  NMR (100 MHz,  $\text{CDCl}_3$ ):  $\delta$  22.0, 23.6, 24.6, 25.8, 29.0, 49.9, 56.1, 104.5, 107.4, 109.5, 111.7, 117.5, 118.4, 122.0, 122.8, 125.0, 125.3, 126.2, 134.8, 138.8, 143.0, 146.8, 148.1, 152.8, 153.9, 161.3 (Figures S9–S12 in Supplementary file). IR ( $\text{cm}^{-1}$ ): 3081, 2962, 1521 ( $\text{NO}_2$ -asymm.), 1343 ( $\text{NO}_2$ -symm.). MS  $m/z$  (%): 493 ( $\text{M} + \text{H}^+$ , 100). Anal. Calcd for  $\text{C}_{26}\text{H}_{25}\text{ClN}_4\text{O}_4$  (492.95): C 63.35, H 5.11, N 11.37. Found: C 63.01, H 4.93, N 12.08. HRMS (ESI TOF):  $[\text{M} + \text{H}]^+$  found 493.1639.  $[\text{C}_{26}\text{H}_{26}\text{ClN}_4\text{O}_4]^+$  requires 493.1637.

1',1',3'-Trimethyl-6-[(E)-4-(nitrophenyl)diazenyl]-1',3,3',4-tetrahydrospiro[chromene-2,2'-benz[e][2H]indole] (7e): Rf = 0.17 (hexane/acetone 10:1,  $v/v$ ), dark brown crystals, yield 1.003 g (42%), mp 199–201 °C.  $^1\text{H}$  BMR (400 MHz,  $\text{CDCl}_3$ ):  $\delta$  1.49 (s, 3H,  $3'$ - $\text{CH}_3$ ), 1.66 (s, 3H,  $3'$ - $\text{CH}_3$ ), 2.31–2.55 (m, 2H, 3- $\text{CH}_2$ ), 2.98 (s, 3H, N- $\text{CH}_3$ ), 3.05–3.31 (m, 2H, 4- $\text{CH}_2$ ), 6.85 (d,  $J = 8.8$  Hz, 1H, 8-H), 7.04 (d,  $J = 8.4$  Hz, 1H,  $4'$ -H), 7.23 (t,  $J = 6.8$  Hz, 1H,  $7'$ -H), 7.41 (t,  $J = 6.8$  Hz, 1H,  $8'$ -H), 7.76–7.82 (m, 4H,  $9'$ -H,  $5'$ -H,  $6'$ -H, 7-H), 7.93–7.98 (m, 3H,  $2''$ -H,

6''-H, 5-H), 8.36 (d,  $J = 8.2$  Hz, 2H, 3''-H, 5''-H).  $^{13}\text{C}$  BMR (100 MHz,  $\text{CDCl}_3$ ):  $\delta$  23.1, 23.7, 23.9, 24.6, 29.2, 51.7, 104.4, 110.5, 121.4, 121.7, 122.0, 123.1 ( $2 \times \text{C}$ ), 124.3, 124.9 ( $2 \times \text{C}$ ), 126.0, 126.5, 129.4, 129.6, 129.8, 129.9, 146.4, 146.6, 148.2, 156.3, 160.9 (Figures S13–S16 in Supplementary file). IR ( $\text{cm}^{-1}$ ): 3055, 2970, 1520 ( $\text{NO}_2$ -asymm.), 1344 ( $\text{NO}_2$ -symm.). Anal. Calcd for  $\text{C}_{29}\text{H}_{26}\text{N}_4\text{O}_3$  (478.54): C 72.79, H 5.48, N 11.71. Found: C 73.10, H 5.43, N 11.64. HRMS (ESI TOF):  $[\text{M} + \text{H}]^+$  found 479.2083.  $[\text{C}_{29}\text{H}_{27}\text{N}_4\text{O}_3]^+$  requires 479.2078.

6'-[(E)-(2-Chloro-4-nitrophenyl)diazenyl]-1',1',3'-trimethyl-1',3,3',4-tetrahydrospiro[chromene-2,2'-benz[e][2H]indole] (7f):  $R_f = 0.16$  (hexane/acetone 10:1,  $v/v$ ), dark brown crystals, yield 1.766 g (69%), mp 200–202 °C.  $^1\text{H}$  BMR (400 MHz,  $\text{CDCl}_3$ ):  $\delta$  1.44–1.70 (m, 6H,  $2 \times 3'$ -CH<sub>3</sub>), 2.47 (br.s, 2H, 3-CH<sub>2</sub>), 2.98 (s, 3H, N-CH<sub>3</sub>), 3.09–3.26 (m, 2H, 4-CH<sub>2</sub>), 6.85 (d,  $J = 8.0$  Hz, 1H, 8-H), 7.04 (d,  $J = 8.8$  Hz, 1H, 4'-H), 7.23 (t,  $J = 7.4$  Hz, 1H, 7'-H), 7.41 (t,  $J = 7.4$  Hz, 1H, 8'-H), 7.71–7.84 (m, 5H, 9'-H, 5'-H, 6'-H, 5-H, 7-H), 7.96 (d,  $J = 8.8$  Hz, 1H, 6''-H), 8.18 (dd,  $J = 8.8$  Hz,  $J = 2.4$  Hz, 1H, 5''-H), 8.42 (d,  $J = 2.4$  Hz, 1H, 3''-H).  $^{13}\text{C}$  BMR (100 MHz,  $\text{CDCl}_3$ ):  $\delta$  23.4, 23.6, 23.7, 24.6, 29.1, 51.7, 104.6, 110.6, 117.4, 118.4 ( $2 \times \text{C}$ ), 121.4, 121.7, 122.1, 122.8 ( $2 \times \text{C}$ ), 125.2, 126.2 ( $2 \times \text{C}$ ), 126.5, 129.5, 129.6, 129.8, 129.9, 134.8, 146.8, 148.1, 152.7, 161.5 (Figures S17 and S18 in Supplementary file). IR ( $\text{cm}^{-1}$ ): 3051, 2978, 1522 ( $\text{NO}_2$ -asymm.), 1343 ( $\text{NO}_2$ -symm.). Anal. Calcd for  $\text{C}_{29}\text{H}_{25}\text{ClN}_4\text{O}_3$  (512.97): C 67.90, H 4.91, N 10.92. Found: C 68.07, H 4.81, N 10.78. HRMS (ESI TOF):  $[\text{M} + \text{H}]^+$  found 513.1698.  $[\text{C}_{29}\text{H}_{26}\text{ClN}_4\text{O}_3]^+$  requires 513.1702.

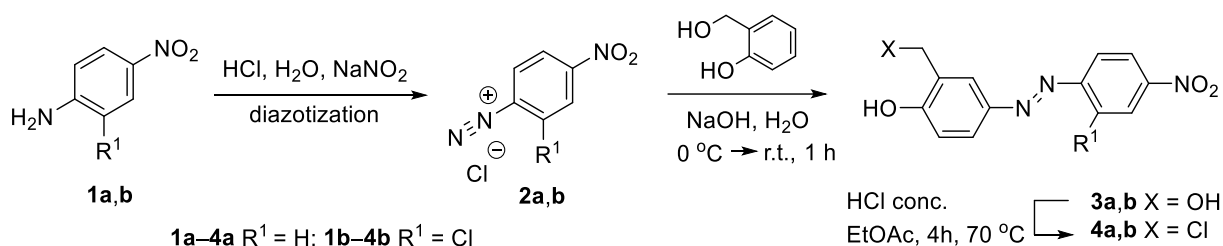
## 2.2. Analytical Procedure

UV–Vis absorption measurements for compounds 7a–f were performed after dissolving them in a mixture of phosphate buffer ( $\text{Na}_2\text{HPO}_4/\text{NaH}_2\text{PO}_4$ , 7.5 mM, pH 7.6) with acetonitrile (19:1,  $v/v$ ) at 298 K. A spectrophotometer quartz cell (0.5 cm light path length) to which prepared solutions were transferred and 0.025  $\text{cm}^3$  of 72 mM sodium cyanide solution was added and was used for the measurements. The absorption was measured against a blank  $\text{CH}_3\text{CN}$ /phosphate buffer from 200 to 700 nm. A sodium cyanide stock solution with a 72 mM concentration was prepared from sodium cyanide and was diluted to concentrations of 36 mM, 3.6 mM, and 0.72 mM. Calibration plots of the most sensitive absorption at 541 nm for 7e versus cyanide concentration were constructed by adding cyanide solutions of 0.72 mM, 3.6 mM, and 36 mM to a 100  $\text{cm}^3$  0.1 mM solution 7e in a  $\text{CH}_3\text{CN}$ /phosphate buffer. All of the volume that was added during titration was negligible (at the most 0.525  $\text{cm}^3$ ) compared to the initial volume of solution 7e.

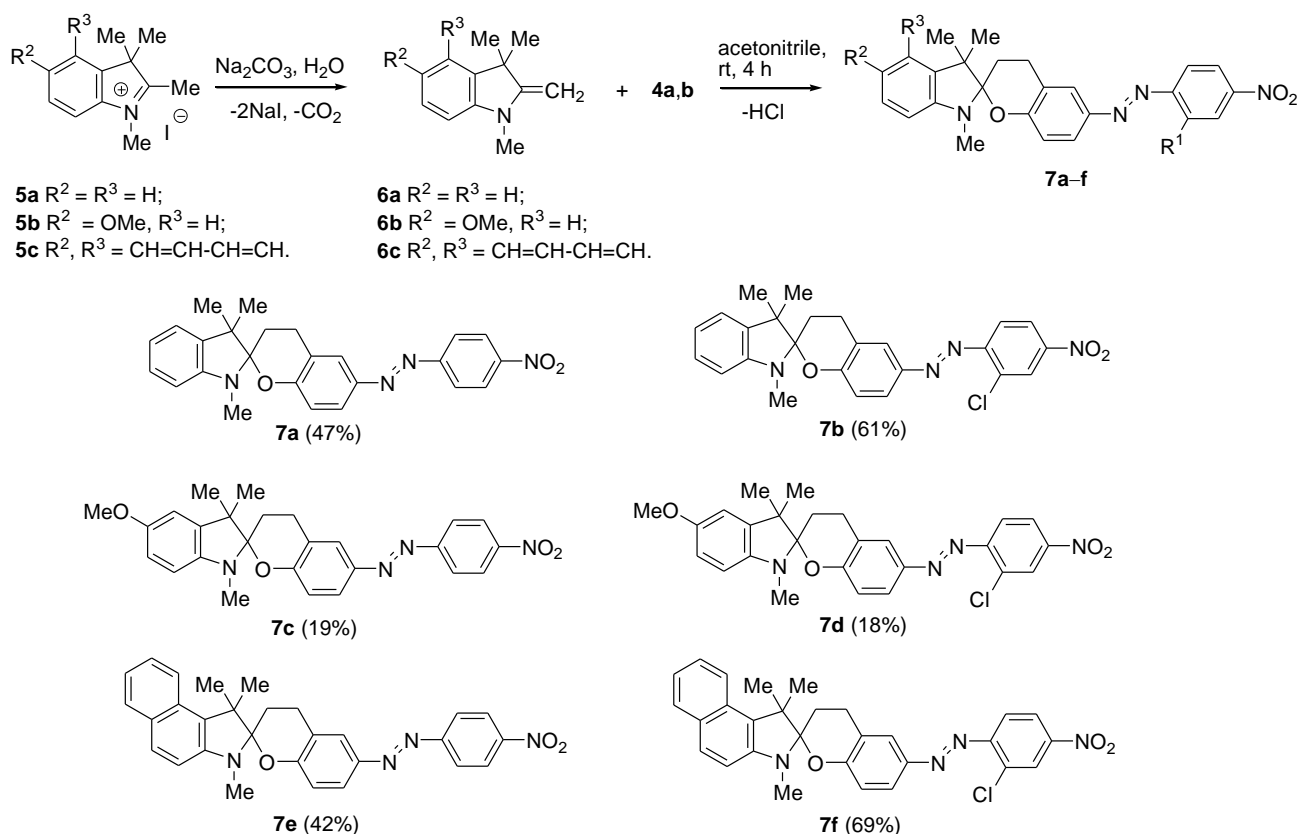
## 3. Results and Discussion

### 3.1. Synthesis

The synthesis strategy for the target compounds 7a–f is outlined in Schemes 1 and 2. The synthesis strategy was based on the reaction of indole enamine 6 with the alkylating agents 2-chloromethyl-4-[(E)-4'-nitrophenyldiazenyl]phenols 4a,b (Scheme 2).



Scheme 1. Synthesis of alkylating agents 4a and 4b.



**Scheme 2.** Synthesis of chemosensors **7a–f**.

The alkylating agents **4** were prepared to start from a diazotization reaction of the anilines **1** and the coupling of the formed 4-nitrophenyldiazonium salts **2** with salicyl alcohol and the subsequent heating of the formed azocompounds **3** with concentrated hydrochloric acid in ethylacetate at 70 °C (Scheme 1).

Indole enamines **6a–c** were obtained from the corresponding 3*H*-indolium salts **5a–c** after treating them with sodium carbonate. The alkylation of the enamines **6** with the derivatives of the diphenyldiazene **4a,b**, which possess a chloromethyl functional group, yielded the formation of 1',3,3',4-tetrahydrospiro[chromene-2,2'-indoles] **7a–f**, which possesses a 4-nitrophenyldiazanyl substituent. The structures of the target compound **7a–f** were proofed by spectroscopic methods. Specific signals of methyl groups were observed in the <sup>1</sup>H NMR spectra. Nevertheless, structures **7a–f** are chiral, two geminal methyls at C-3' carbon atom produce singlets at 1.27–1.29 ppm, and the N-CH<sub>3</sub> groups produced singlets at 2.82–2.89 ppm. The singlet of geminal methyls can be explained by a quick dihydropyran ring-closing–opening equilibrium, which was proven earlier [24]. The signals at 103.8–104.6 ppm in the <sup>13</sup>C NMR spectra of compounds **7a–f** were attributed to spiro-carbon atoms.

### 3.2. UV–Vis Spectral Investigations and Chemosensing Mechanism

It is known that 1',3,3',4-tetrahydrospiro[chromene-2,2'-indoles] are sensitive to cyanides and that, upon their action, these chemosensors become yellow in color due to the opening of a partially saturated pyran ring and the formation of a 4-nitrophenolate chromophore [25]. The attachment of the 4-nitrophenyldiazanyl substituent to the main core of the molecule lengthens the conjugated  $\pi$ -electron system and expands the color palette of the opened form.

Steady-state absorption spectra of compounds **7a–f**, which were measured for the solutions in CH<sub>3</sub>CN/phosphate buffer, revealed modest absorption in the visible parts of the electronic spectra (Table 1). The absorption spectra of the chemosensors possessing a Cl substituent in their structures (**7b**, **7d**, and **7f**) have the maxima of the absorption at approximately 393 nm, and the solutions appear more yellowish in color than the corresponding sensor solutions without the Cl substituent (**7a**, **7c**, and **7e**), the maxima of which are at approximately 384 nm. However, when a NaCN solution buffered with sodium phosphate (pH 7.6) was added to the aforementioned solutions of compounds **7a–f**, a new absorption band appeared in the visible area at approximately 540 nm for **7a**, **7c**, and **7e** and at approximately 570 nm for **7b**, **7d**, and **7f** (Table 1, Figure 1), which was observed by the naked eye as the color changed from yellow to magenta and blue.

**Table 1.** Data of UV–Vis absorption spectra for compounds **7** and **8**<sup>1</sup>.

Entry	Compound	$\lambda_{\max}$ of <b>7</b> (nm)	$\epsilon \times 10^3$ (dm <sup>3</sup> ·mol <sup>-1</sup> ·cm <sup>-1</sup> )	Compound	$\lambda_{\max}$ of <b>8</b> (nm)	$\epsilon \times 10^3$ (dm <sup>3</sup> ·mol <sup>-1</sup> ·cm <sup>-1</sup> )
1	<b>7a</b>	203	56.5	<b>8a</b>	201	57.2
		242	39.0		247	16.6
		385	29.8		290	13.0
					370	6.2
2	<b>7b</b>	205	59.9	<b>8b</b>	<b>544</b>	38.8
		241	19.4		202	57.4
		393	27.2		246	15.4
					291	12.4
3	<b>7c</b>	240	16.4	<b>8c</b>	<b>574</b>	43.8
		383	22.2		246	14.3
					296	10.2
					<b>546</b>	31.6
4	<b>7d</b>	204	49.4	<b>8d</b>	203	50.0
		240	16.4		245	14.0
		316	8.8		300	10.6
		394	18.4		<b>579</b>	34.0
5	<b>7e</b>	214	39.8	<b>8e</b>	206	40.2
		247	60.8		249	56.2
		291	13.6		290	56.6
		298	13.0		298	15.6
6	<b>7f</b>	382	23.0	<b>8f</b>	357	9.0
					<b>541</b>	34.4
		205	39.6		208	41.4
		247	51.2		249	45.2
		292	14.0		290	1.2
		307	11.4		300	13.0
		351	5.6			
		392	21.8	<b>573</b>	36.4	

<sup>1</sup> Spectra were recorded for solutions of compounds **7** in mixture of CH<sub>3</sub>CN/phosphate buffer (Na<sub>2</sub>HPO<sub>4</sub>/NaH<sub>2</sub>PO<sub>4</sub>, 7.5 mM, pH 7.6) (19:1, v/v) at 298 K without CN<sup>-</sup> ions and after addition of CN<sup>-</sup> ions and complete formation of forms **8**.



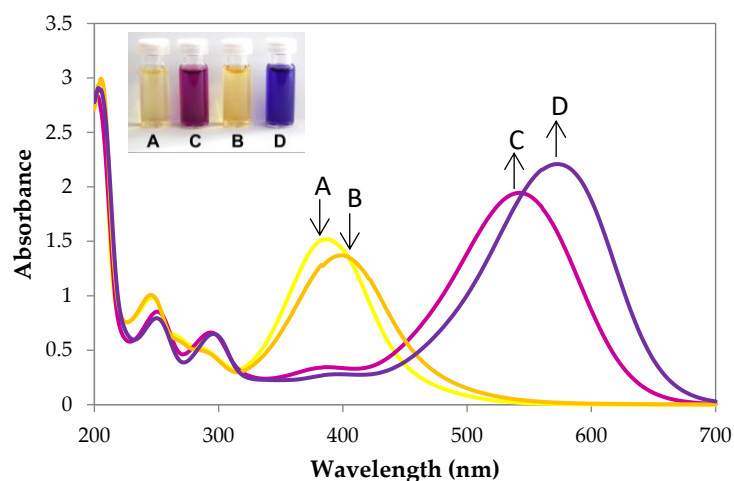
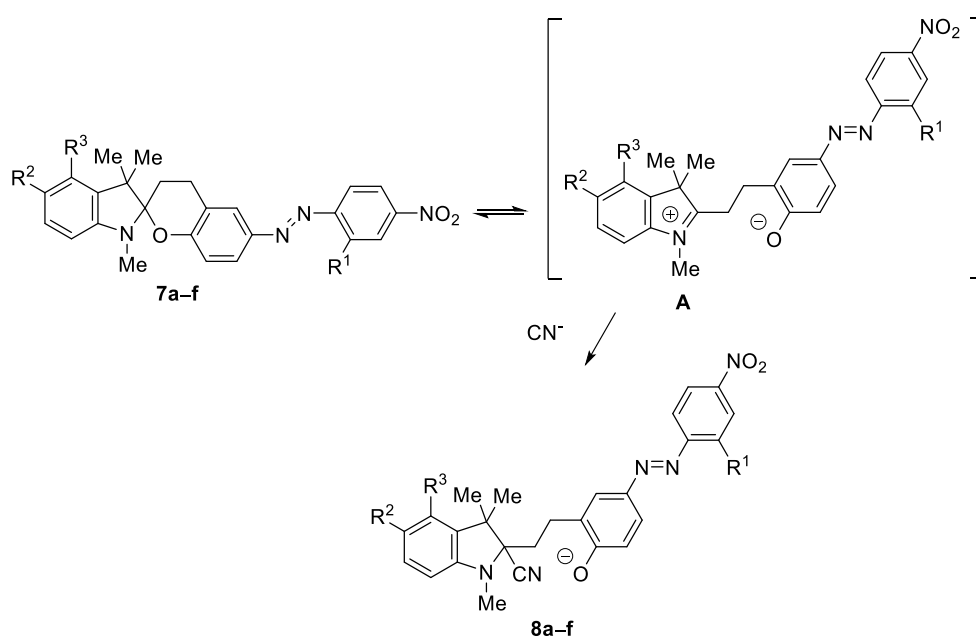


**Figure 1.** Absorption spectra of **7a** and **7b** (0.1 mM, 298 K) in a mixture of  $\text{CH}_3\text{CN}$ /phosphate buffer ( $\text{Na}_2\text{HPO}_4/\text{NaH}_2\text{PO}_4$ , 7.5 mM, pH 7.6) (19:1,  $v/v$ ) (spectra A and B) and with added  $\text{NaCN}$  (10 equiv, spectra C and D, respectively).

The almost complete disappearance of the absorption bands at approximately 400 nm and the appearance of new absorption bands at approximately 540 nm and 570 nm can be rationalized by the spirochromane ring opening and the formation of 4-(4-nitrophenyldiazenyl)phenolate chromophores in structures **8a–f**. This occurs immediately when cyanide anion nucleophilically substitutes pyranic oxygen at the C-2 atom of the indole ring. The reaction rate depends on the ease of dissociation of the  $\text{C}_{(\text{spiro})}\text{-O}$  covalent bond and the formation of zwitterionic intermediates **A**, which are in an equilibrated mixture with the starting 6-[(*E*)-(4-nitrophenyl)diazenyl]-1',3,3',4-tetrahydrospiro[chromene-2,2'-indoles] **7a–f**.

After the nucleophilic addition of the cyanide anion to the C-2 carbon atom of the indolium moiety, stable nitriles **8a–f** form. In such cases, the equilibrium ring-opening–closing reaction of **7a–f** becomes irreversible (Scheme 3).



**Scheme 3.** Formation of 4-(4-nitrophenyldiazenyl)phenolate chromophore **8a–f**.

The covalent character of the bond between the C-2 carbon atom and the carbon atom of the nitrile group was shown earlier by NMR spectroscopy [25] and was confirmed by a mass spectra experiment for **7c** (Figure 2).



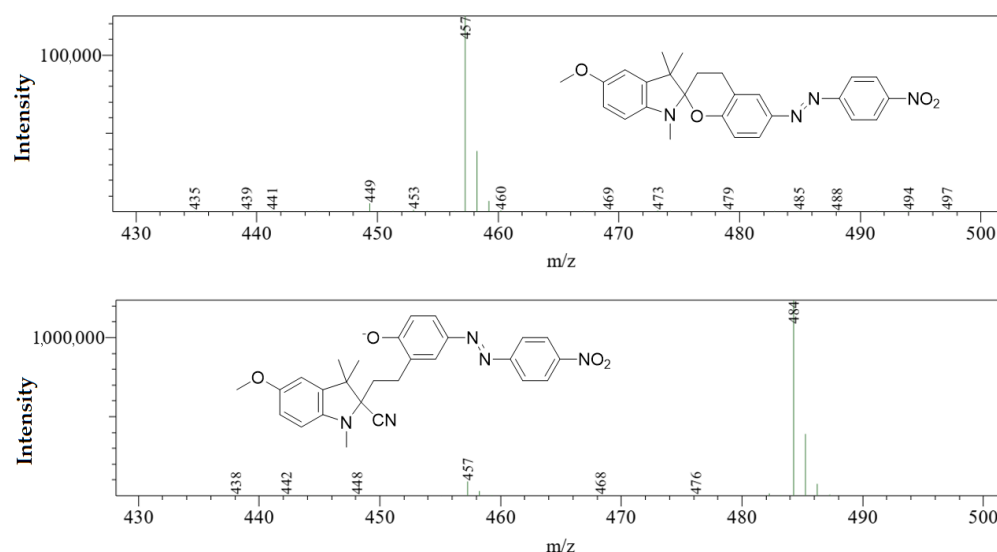


**Figure 2.** Mass spectrum of **7c** in a mixture of  $\text{CH}_3\text{CN}$ /phosphate buffer ( $\text{Na}_2\text{HPO}_4/\text{NaH}_2\text{PO}_4$ , 7.5 mM, pH 7.6) (19:1,  $v/v$ ) before (A) and after (B) the addition of NaCN of NaCN (2.5 equiv, ESI(-)).

Parallel investigations were carried out to test the selectivity of the chemosensor **7e** with a series of other anions. The addition of excess amounts of the other anions did not cause significant absorbance spectral changes during UV–Vis titration (Figure 3), except hydrocarbonate and sulfite anions. This indicates that investigated anions do not compete with the cyanide in the addition reaction to the C-2 carbon atom making a covalent bond with the indole nucleus, neither yielding colored phenolate **8**, because they do not form a covalent bond to the mentioned atom. To avoid hydrocarbonate interaction, the analyte should be heated at boiling temperature for 5 min, to decompose hydrocarbonate. Sulfites are not usually present in natural water. If there is a sample of technological water, in which sulfites are present, actions for evaluation of sulfite concentration must be done, to avoid misinterpretation of cyanide analysis data.

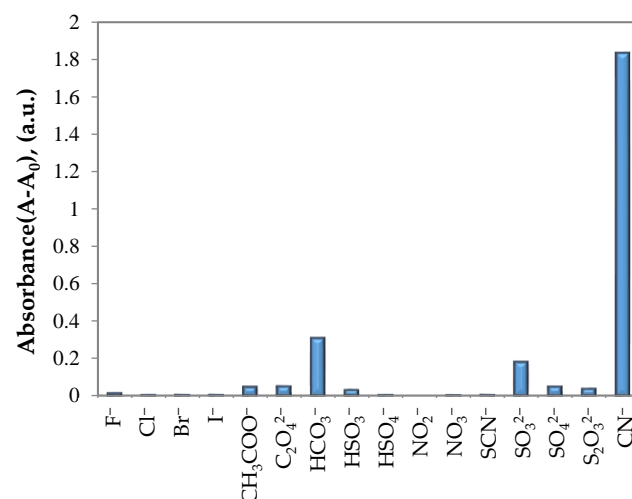


**Figure 3.** Absorbance of **7e** (0.1 mM, 298 K) at 541 nm in mixture of  $\text{CH}_3\text{CN}$ /phosphate buffer ( $\text{Na}_2\text{HPO}_4/\text{NaH}_2\text{PO}_4$ , 7.5 mM, pH 7.6) (19:1,  $v/v$ ) in the presence of  $\text{CN}^-$  or other anions (10 equiv), where  $A_0$  is the absorbance of **7e** at 541 nm in the absence of  $\text{CN}^-$ .

To measure the speed at which the chemosensors **7** change color, dynamic colorimetric measurements at the corresponding absorption maxima in the visible spectrum of the mixtures of compounds **7a–f** with cyanide ions were performed (Figure 4). Compounds **7c** and **7d**, which possessed a methoxy group at the C-5 carbon atom of the indole ring, had

the quickest response time to the cyanide ions, approximately 20 s. This can be rationalized by the fact that the methoxy group donates electrons and stabilizes the indolium cation, and subsequently, the formation of **8c** and **8d** becomes easier and quicker (Scheme 3).

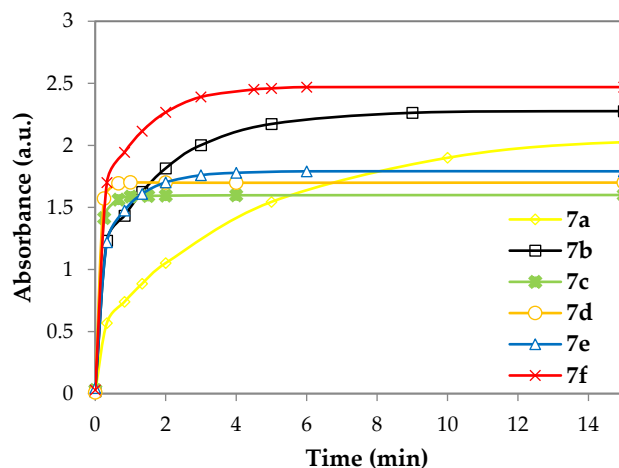


**Figure 4.** Absorbance changes for **7a–f** (0.1 mM, 298 K) at 544, 574, 546, 579, 541, and 573 nm, respectively, in a mixture of CH<sub>3</sub>CN/phosphate buffer (Na<sub>2</sub>HPO<sub>4</sub>/NaH<sub>2</sub>PO<sub>4</sub>, 7.5 mM, pH 7.6) (19:1, *v/v*) after the addition of NaCN (10 equiv).

To test the potential applications of chemosensor **7e** for the quantitative determination of CN<sup>−</sup> ions, a calibration curve of the cyanide concentration versus the absorption at 541 nm was plotted (Figure 5) (deviations in Table S1 in Supplementary file). The curve shows that this chemosensor is sensitive to relatively low concentrations of CN<sup>−</sup> in acetonitrile/phosphate buffer solution.

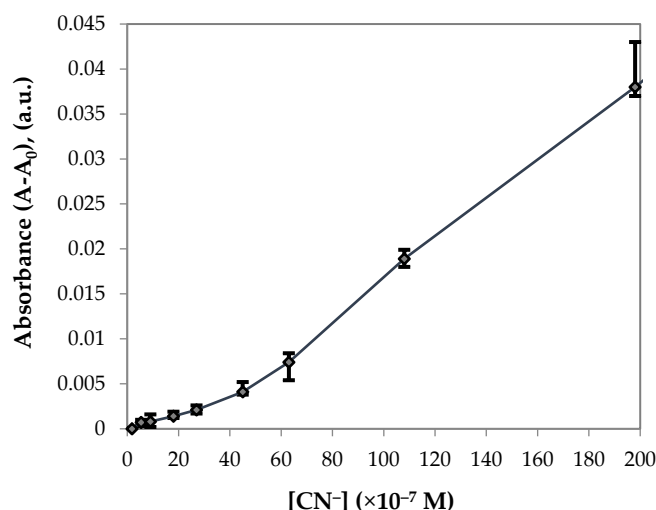


**Figure 5.** Absorbance of **7e** at 541 nm (0.1 mM, 298 K) in a mixture of CH<sub>3</sub>CN/phosphate buffer (Na<sub>2</sub>HPO<sub>4</sub>/NaH<sub>2</sub>PO<sub>4</sub>, 7.5 mM, pH 7.6) (19:1, *v/v*) in the presence of different concentrations of CN<sup>−</sup>, where A<sub>0</sub> is the absorbance of **7e** at 541 nm in the absence of CN<sup>−</sup>.

#### 4. Conclusions

The derivatives of 1',3,3',4-tetrahydrospiro[chromene-2,2'-indole] possessing a 4-nitrophenyldiazenyl moiety were synthesized. These substances undergo transformations to the colored ring-open form, which possess the 4-nitrophenyldiazenylphenolate chromophore when treated with cyanide in an acetonitrile solution buffered with sodium phosphate. The transformation is accompanied by a quick and distinct color change from orange to magenta and blue, which can be measured colorimetrically or can be easily

detected by the naked eye. These new compounds are not sensitive to halides, which often interfere with cyanides. Their high sensitivity to low concentrations (<0.05 mg/L) of cyanide anions and quick development of color (up to tens of seconds) make them attractive as potential colorimetric or naked-eye chemosensors.

**Supplementary Materials:** The following supporting information can be downloaded at: <https://www.mdpi.com/article/10.3390/chemosensors10050185/s1>, Figure S1:  $^1\text{H}$  NMR spectra of 4-[(E)-2-Chloro-4'-nitrophenyl]diazanyl-2-hydroxymethylphenol (**3b**). Figure S2:  $^{13}\text{C}$  NMR spectra of 4-[(E)-2-Chloro-4'-nitrophenyl]diazanyl-2-hydroxymethylphenol (**3b**). Figure S3:  $^1\text{H}$  NMR spectra of 1',3',3'-Trimethyl-6-[(E)-(4-nitrophenyl)diazanyl]-1',3,3',4-tetrahydrospiro[chromene-2,2'-indole] (**7a**). Figure S4:  $^{13}\text{C}$  NMR spectra of 1',3',3'-Trimethyl-6-[(E)-(4-nitrophenyl)diazanyl]-1',3,3',4-tetrahydrospiro[chromene-2,2'-indole] (**7a**). Figure S5:  $^1\text{H}$  NMR spectra of 6-[(E)-(2-Chloro-4-nitrophenyl)diazanyl]-1',3',3'-trimethyl-1',3,3',4-tetrahydrospiro[chromene-2,2'-indole] (**7b**). Figure S6:  $^{13}\text{C}$  NMR spectra of 6-[(E)-(2-Chloro-4-nitrophenyl)diazanyl]-1',3',3'-trimethyl-1',3,3',4-tetrahydrospiro[chromene-2,2'-indole] (**7b**). Figure S7:  $^1\text{H}$  NMR spectra of 5'-Methoxy-1',3',3'-trimethyl-6-[(E)-(4-nitrophenyl)diazanyl]-1',3,3',4-tetrahydrospiro[chromene-2,2'-indole] (**7c**). Figure S8:  $^{13}\text{C}$  NMR spectra of 5'-Methoxy-1',3',3'-trimethyl-6-[(E)-(4-nitrophenyl)diazanyl]-1',3,3',4-tetrahydrospiro[chromene-2,2'-indole] (**7c**). Figure S9:  $^1\text{H}$  NMR spectra of 6-[(E)-(2-Chloro-4-nitrophenyl)diazanyl]-5'-methoxy-1',3',3'-trimethyl-1',3,3',4-tetrahydrospiro[chromene-2,2'-indole] (**7d**). Figure S10:  $^{13}\text{C}$  NMR spectra of 6-[(E)-(2-Chloro-4-nitrophenyl)diazanyl]-5'-methoxy-1',3',3'-trimethyl-1',3,3',4-tetrahydrospiro[chromene-2,2'-indole] (**7d**). Figure S11:  $^1\text{H}$ - $^1\text{H}$  COSY NMR spectra of 6-[(E)-(2-Chloro-4-nitrophenyl)diazanyl]-5'-methoxy-1',3',3'-trimethyl-1',3,3',4-tetrahydrospiro[chromene-2,2'-indole] (**7d**). Figure S12:  $^1\text{H}$ - $^{13}\text{C}$  HSQC NMR spectra of 6-[(E)-(2-Chloro-4-nitrophenyl)diazanyl]-5'-methoxy-1',3',3'-trimethyl-1',3,3',4-tetrahydrospiro[chromene-2,2'-indole] (**7d**). Figure S13:  $^1\text{H}$  NMR spectra of 1',1',3'-Trimethyl-6-[(E)-4-(nitrophenyl)diazanyl]-1',3,3',4-tetrahydrospiro[chromene-2,2'-benz[e][2H]indole] (**7e**). Figure S14:  $^{13}\text{C}$  NMR spectra of 1',1',3'-Trimethyl-6-[(E)-4-(nitrophenyl)diazanyl]-1',3,3',4-tetrahydrospiro[chromene-2,2'-benz[e][2H]indole] (**7e**). Figure S15:  $^1\text{H}$ - $^1\text{H}$  COSY NMR spectra of 1',1',3'-Trimethyl-6-[(E)-4-(nitrophenyl)diazanyl]-1',3,3',4-tetrahydrospiro[chromene-2,2'-benz[e][2H]indole] (**7e**). Figure S16:  $^1\text{H}$ - $^{13}\text{C}$  HSQC NMR of 1',1',3'-Trimethyl-6-[(E)-4-(nitrophenyl)diazanyl]-1',3,3',4-tetrahydrospiro[chromene-2,2'-benz[e][2H]indole] (**7e**). Figure S17:  $^1\text{H}$  NMR of 6'-[(E)-(2-Chloro-4-nitrophenyl)diazanyl]-1',1',3'-trimethyl-1',3,3',4-tetrahydrospiro[chromene-2,2'-benz[e][2H]indole] (**7f**). Figure S18:  $^{13}\text{C}$  NMR spectra of 6'-[(E)-(2-Chloro-4-nitrophenyl)diazanyl]-1',1',3'-trimethyl-1',3,3',4-tetrahydrospiro[chromene-2,2'-benz[e][2H]indole] (**7f**). Table S1: Data for plotting calibration curve.

**Author Contributions:** M.D. and G.M. were responsible for synthesis experiments and data analysis; S.K. was responsible for colorimetric measurements and data analysis; A.Š. and V.M. for writing the article and editing. All authors have read and agreed to the published version of the manuscript.

**Funding:** This research was funded by grant No. MIP-022/2013 from the Research Council of Lithuania and The Doctoral Fund of Kaunas University of Technology No. A-410, approved 26 June 2019.

**Institutional Review Board Statement:** Not applicable.

**Informed Consent Statement:** Not applicable.

**Conflicts of Interest:** The authors declare no conflict of interest.

## References

1. Alberts, B.; Johnson, A.; Lewis, J.; Morgan, D.; Raff, M.; Roberts, K.; Walter, P. *Molecular Biology of the Cell*; Garland Science, Taylor & Francis Group, LLC: New York, NY, USA, 2015; p. 772. [\[CrossRef\]](#)
2. Aranguri-Llerena, G.; Siche, R. Superior Plants with Significant Amounts of Cyanide and Their Toxicological Implications. *Rev. Agric. Sci.* **2020**, *8*, 354–366. [\[CrossRef\]](#)
3. Dolan, L.C.; Matulka, R.A.; Burdock, G.A. Naturally Occurring Food Toxins. *Toxins* **2010**, *2*, 2289–2332. [\[CrossRef\]](#) [\[PubMed\]](#)
4. Lawson-Smith, P.; Jansen, E.C.; Hyldegaard, O. Cyanide intoxication as part of smoke inhalation—a review on diagnosis and treatment from the emergency perspective. *Scand. J. Trauma Resusc.* **2011**, *19*, 14. [\[CrossRef\]](#)
5. Xu, Z.; Chen, X.; Kim, H.N.; Yoon, J. Sensors for the optical detection of cyanide ion. *Chem. Soc. Rev.* **2010**, *39*, 127–137. [\[CrossRef\]](#) [\[PubMed\]](#)

6. Udhayakumari, D. Chromogenic and fluorogenic chemosensors for lethal cyanide ion. A comprehensive review of the year 2016. *Sens. Actuators B Chem.* **2018**, *259*, 1022–1057. [[CrossRef](#)]
7. Erdemir, S.; Malkondu, S. On-site and low-cost detection of cyanide by simple colorimetric and fluorogenic sensors: Smartphone and test strip applications. *Talanta* **2020**, *207*, 120278. [[CrossRef](#)] [[PubMed](#)]
8. Sun, C.; Gradzielski, M. Fluorescence sensing of cyanide anions based on Au-modified upconversion nanoassemblies. *Analyst* **2021**, *146*, 2152–2159. [[CrossRef](#)] [[PubMed](#)]
9. Isaad, J.; Perwuelz, A. New color chemosensors for cyanide based on water soluble azo dyes. *Tetrahedron Lett.* **2010**, *51*, 5810–5814. [[CrossRef](#)]
10. Gong, W.T.; Zhang, Q.L.; Shang, L.; Gao, B.; Ning, G.L. A new principle for selective sensing cyanide anions based on 2-hydroxy-naphthaldeazine compound. *Sens. Actuators B Chem.* **2013**, *177*, 322–326. [[CrossRef](#)]
11. Lee, D.Y.; Singh, N.; Satyender, A.; Jang, D.O. An azo dye-coupled tripodal chromogenic sensor for cyanide. *Tetrahedron Lett.* **2011**, *52*, 6919–6922. [[CrossRef](#)]
12. Ren, J.; Zhu, W.; Tian, H. A highly sensitive and selective chemosensor for cyanide. *Talanta* **2008**, *75*, 760–764. [[CrossRef](#)] [[PubMed](#)]
13. Shiraishi, Y.; Adachi, K.; Itoh, M.; Hirai, T. Spiropyran as a Selective, Sensitive, and Reproducible Cyanide Anion Receptor. *Org. Lett.* **2009**, *11*, 3482–3485. [[CrossRef](#)] [[PubMed](#)]
14. Orojloo, M.; Amani, S. Naked-eye detection of cyanide ions in aqueous media based on an azo-azomethine chemosensor. *Comptes Rendus Chim.* **2017**, *20*, 415–423. [[CrossRef](#)]
15. Bhaskar, R.; Sarveswari, S. Colorimetric sensor for real-time detection of cyanide ion in water and food samples. *Inorg. Chem. Commun.* **2019**, *102*, 83–89. [[CrossRef](#)]
16. Morikawa, Y.; Nishiwaki, K.; Suzuki, S.; Yasaka, S.; Okada, Y.; Nakanishi, I. A new chemosensor for cyanide in blood based on the Pd complex of 2-(5-bromo-2-pyridylazo)-5-[N-n-propyl-N-(3-sulfopropyl)amino]phenol. *Analyst* **2020**, *145*, 7759–7764. [[CrossRef](#)]
17. Gai, L.; Mack, J.; Lu, H.; Nyokong, T.; Li, Z.; Kobayashi, N.; Shen, Z. Organosilicon compounds as fluorescent chemosensors for fluoride anion recognition. *Coord. Chem. Rev.* **2015**, *285*, 24–51. [[CrossRef](#)]
18. Wang, Y.; Kim, S.H. Colorimetric chemodosimeter for cyanide detection based on spiropyran derivative and its thermodynamic studies. *Dyes Pigm.* **2014**, *102*, 228–233. [[CrossRef](#)]
19. Tomasulo, M.; Raymo, F.M. Colorimetric Detection of Cyanide with a Chromogenic Oxazine. *Org. Lett.* **2005**, *7*, 4633–4636. [[CrossRef](#)]
20. Tomasulo, M.; Sortino, S.; White, A.J.P.; Raymo, F.M. Chromogenic Oxazines for Cyanide Detection. *J. Org. Chem.* **2006**, *71*, 744–753. [[CrossRef](#)]
21. Shao, N.; Zhang, Y.; Cheung, S.; Yang, R.; Chan, W.; Mo, T.; Li, K.; Liu, F. Copper Ion-Selective Fluorescent Sensor Based on the Inner Filter Effect Using a Spiropyran Derivative. *Anal. Chem.* **2005**, *77*, 7294–7303. [[CrossRef](#)]
22. Potisek, S.L.; Davis, D.A.; Sottos, N.R.; White, S.R.; Moore, J.S. Mechanophore-Linked Addition Polymers. *J. Am. Chem. Soc.* **2007**, *129*, 13808–13809. [[CrossRef](#)] [[PubMed](#)]
23. Kiyose, K.; Hanaoka, K.; Oshiki, D.; Nakamura, T.; Kajimura, M.; Suematsu, M.; Nishimatsu, H.; Yamane, T.; Terai, T.; Hirata, Y.; et al. Hypoxia-Sensitive Fluorescent Probes for in Vivo Real-Time Fluorescence Imaging of Acute Ischemia. *J. Am. Chem. Soc.* **2010**, *132*, 15846–15848. [[CrossRef](#)] [[PubMed](#)]
24. Dagilienė, M.; Martynaitis, V.; Vengris, M.; Redekas, K.; Voiciuk, V.; Holzer, W.; Šačkus, A. Synthesis of 1',3,3',4-tetrahydrospiro[chromene-2,2'-indoles] as a new class of ultrafast light-driven molecular switch. *Tetrahedron* **2013**, *69*, 9309–9315. [[CrossRef](#)]
25. Dagilienė, M.; Martynaitis, V.; Kriščiūnienė, V.; Krikštolaitytė, S.; Šačkus, A. Colorimetric Cyanide Chemosensor Based on 1',3,3',4-Tetrahydrospiro[chromene-2,2'-indole]. *ChemistryOpen* **2015**, *4*, 363–369. [[CrossRef](#)]